Merging of Aircraft Trailing Vortices

Steven A. Brandt* and James D. Iversen†
Iowa State University, Ames, Iowa

A merging distance criterion for equal-strength corotational vortices is derived from low-turbulence wind tunnel flow visualization data. The vortex separation distance is normalized by defining a vortex core diameter based on circulation defect and angular momentum defect. Merging may take place for larger separation distances than predicted from earlier two-dimensional inviscid calculations, which indicates that viscosity and possibly three-dimensional effects are important factors in the merging phenomenon. Hot-wire velocity distributions and rolling moment measurements show that attenuation of the vortex hazard is associated with vortex merging.

Nomenclature

b_g = generator wingspan
b_f = follower wingspan
C_L = lift coefficient
c_l = rolling-moment coefficient
c = wing chord
d = vortex separation distance
d_0 = initial vortex separation distance
d_c = vortex core diameter (usually based on peak tangential speed)
d_M = vortex core diameter (based on angular momentum defect equal to that in a Rankine vortex)
d_Γ = vortex core diameter (based on circulation defect equal to that in a Rankine vortex)
d_v = vortex core diameter (based on outer boundary of the rotational portion of the vortex)
r = vortex radial coordinate
r_Γ = $d_\Gamma/2$
S_g = generator wing area
S_f = follower wing area
t = time after vortex formation
U_∞ = freestream speed
x_m = distance from vortex formation to merger
Γ = circulation, $2\pi r$ times tangential speed
Γ_0 = large radius circulation
ν = kinematic viscosity
θ = angular position of vortex pair from formation

Introduction

THE hazard to smaller aircraft caused by the trailing vortices shed from the wings of wide-body jet-transport aircraft is still a problem of considerable concern. Among the many attempts at wake-vortex hazard alleviation,[1] NASA wind tunnel[2] and flight tests[3] have shown that the hazard can be reduced by altering the spanwise lift distribution on the generating aircraft. For example, if an inboard wing flap is deployed, a strong vortex is shed from the outboard edge of the inboard flap as well as one from the wingtip. If these two vortices of like rotational sense are sufficiently close, merging of the two vortices takes place, and a single vortex remains. The vorticity within the resulting single vortex may be sufficiently diffuse that the hazard to trailing aircraft is significantly reduced from that due to conventional wing loading.[2]

The merging of corotational vortices has been studied recently in connection with the trailing vortex hazard and also with the pairing of organized vortex structures observed in turbulent mixing layers. Winant and Browand[4] and Browand and Weidman[5] present photographs of a low-Reynolds-number mixing layer in which the turbulent layer grows by the repetition of the vortex pairing process. In this process, two adjoining vortices in the layer interact to form a single, larger vortex. Moore and Saffman's approximate analysis[6,7] shows that an array of vortices with elliptically shaped cores is unstable to disturbances if the spacing between the vortices is too close. Bilanin et al.[8] extend that analysis to obtain a stability boundary in terms of the ratio of circulation strengths Γ_1/Γ_2, vortex core cross-section shape, and separation distance to core diameter ratio d/d_c. Bilanin et al.[8-10] also show flow-visualization photographs in interacting and merged vortices in a small wind tunnel.

One procedure used to investigate the inviscid merging process has been to represent rotational vortex cores by arrays of two-dimensional line vortices. The Rankine vortex, with constant vorticity core, was approximately represented in this manner by Christiansen and co-authors[11-13] and by Rossow.[14,15] Christiansen obtained a critical relative separation distance d/d_c of 1.7 for equal-strength Rankine vortices. For larger separation distances, the two corotating vortices rotate about each other but do not merge. Rossow[14] presents critical separation distances for two vortices of various relative strengths and for circulation profile functions other than Rankine. The critical separation distance for a vortex profile, which is approximately Rankine (but more approximate than Christiansen's model since far fewer line vortices were used), is about 10% larger than 1.7. A finite difference approach was utilized by Steger and Kutler[16] to approximately verify Rossow's inviscid merging boundary curve. However, the initial vortex shape they used was a Lamb vortex profile, rather than a Rankine or any other of Rossow's profiles.

To increase the understanding of the vortex merging phenomenon, experimental research has been initiated in the Iowa State University low-turbulence open-circuit wind tunnel. Flow visualization and hot-wire anemometer measurements have been used to determine qualitative and quantitative data for single, interacting, and merged vortices. Two vortices were generated by semispan wing models inserted through opposite or adjacent walls of the wind tunnel test section. A similitude relationship for merging distances is derived, based on flow visualization experiments, which is shown to condense merging distance data to a single curve. Hot-wire anemometer mean speed measurements in interacting and merged vortices and rolling moment measurements on a following model are also presented.

Received Jan. 13, 1977; presented as Paper 77-8 at the AIAA 15th Aerospace Sciences Meeting, Los Angeles, Calif., Jan 24-26, 1977; revision received June 23, 1977.

Index categories: Jets, Wakes, and Viscid-Inviscid Flow Interactions; Viscous Nonboundary-Layer Flows.

*Graduate Research Assistant, Department of Aerospace Engineering.

†Professor, Department of Aerospace Engineering. Associate Fellow AIAA.

Circulation Defect Diameter

Rossow's[14] mention of a difference for critical separation distance of equal strength vortices between his and Christiansen's result for the approximated Rankine vortex (1.9–1.7) led to the consideration of the possibility of a "universal" normalizing reference diameter in order to compare merging characteristics for various vortex pair circulation profiles. Several possible reference diameters were tried, including equating the defects of circulation and angular momentum within an arbitrary vortex to that within a Rankine vortex of core diameter d_Γ or d_M. Rossow normalized the initial critical separation distance by dividing that distance by a core diameter d_v, which, for the arbitrary vortex profile, is the outer boundary of the rotational portion of the vortex. For different circulation functions for the rotational vortex core, he obtained different critical merging boundary curves. The use of either circulation defect or angular momentum defect serves to approximately coalesce Rossow's boundary curves (Fig. 8 of Ref. 14). If the defect in circulation for an arbitrary vortex (for which circulation $\Gamma < \Gamma_0$ for radius $r < d_v/2$) is equated to the defect in circulation for a Rankine vortex ($\Gamma = \Gamma_0(1 - r^2/r_\Gamma^2)$), the following equation results:

$$d_\Gamma = 3\int_0^{r_v}\left(1 - \frac{\Gamma}{\Gamma_0}\right) dr \qquad (1a)$$

Equating the integral of defect in circulation of the two vortices is equivalent to equating the area integral of the first moment of vorticity. If the defect in angular momentum for an arbitrary vortex is equated to the defect in angular momentum for a Rankine vortex of core radius r_M, an equation of angular momentum defect results:

$$d_M = 4\left[\int_0^{r_v}\left(1 - \frac{\Gamma}{\Gamma_0}\right) r dr\right]^{1/2} \qquad (1b)$$

Use of Eq. (1b) is equivalent to equating the area integral of the second moment of vorticity.

Rossow's merging boundary curves are replotted in Figs. 1a and b, with d_Γ and d_M as the normalizing distances instead of d_v. Although the curves do not completely coalesce, the range of normalized separation distances for a given circulation ratio is considerably reduced. Rossow's range of k (from -1 to 2) represents members of a family of circulation profiles that differ widely in shape. The straining field that each vortex exerts on the other is thus quite different for $k = -1$ than it is for $k = 2$ for equal values of d_0 and d_v. The diameter d_M is linearly proportional to the radius of gyration of the vorticity. Intuitively it might be expected that the mutual influence would be similar for two systems of two vortices of like diameter d_M and not for two systems of the same d_v but different d_M. That, at least, can be inferred from the results in Fig. 1b. It is not clear why normalization by d_M makes so little difference from normalization by d_Γ. For the Rankine vortex (Rossow's $k = 0$), the critical separation distances for equal strength vortices are $d/d_\Gamma = 1.72$ and $d/d_M = 1.69$, in good agreement with Christiansen's value of 1.7.

Test Equipment and Procedure

Tests were conducted in the Iowa State University Aerospace Engineering Department's open-circuit low-turbulence (0.1%) wind tunnel. The test section length is adjustable from 6 to 28 ft; the cross section is 36.55×30.0 in.; and the maximum velocity is slightly over 200 fps. A traversing mechanism, on which hot-wire anemometer probes or rolling moment models can be mounted, is located at the downstream end of the test section. Two TSI 1054A linearized, hot-wire anemometers with a cross-wire probe were used for velocity measurements.

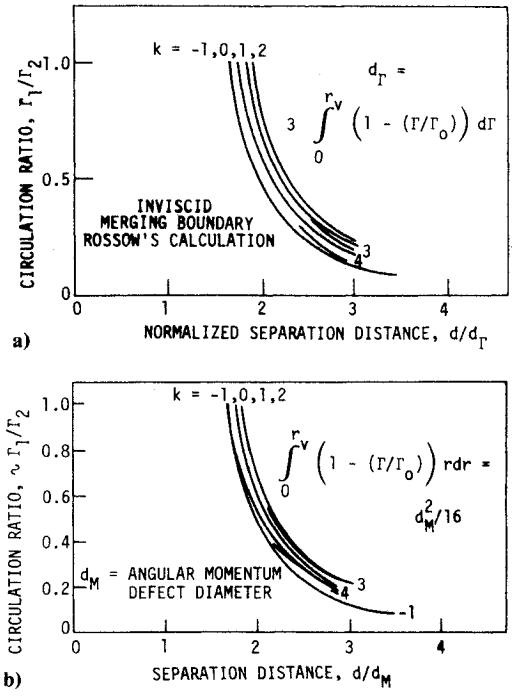

Fig. 1 Merging boundary curves of Rossow[14] normalized by a) circulation defect diameter and b) angular momentum defect diameter.

The vortices were made visible by injecting steam into the flow, either through holes in the underside of the wing models near the tip or through a rake upstream of the tunnel inlet. When temperatures were above 45°F and relative humidities below 75%, the steam was made visible by injecting liquid nitrogen into the flow with it.

To better observe the structure and motions of the vortex system, the test section was illuminated with a series of light slits, resulting in a series of cross sections of the flow at discrete streamwise locations. By rotating the slits 30–45 deg and placing a camera outside the test section in the proper location to cancel the distortion caused by the rotation, photographs were made that showed successive streamwise cross sections side by side. Figure 2 is an example of one such photograph. This procedure permits the entire merging process to be recorded on one photograph. For purposes of pinpointing a particular spot in the flow, multiple or single slits could be moved streamwise.

Wing models of variable semispan, inserted through adjacent or opposite sides of the test section at the same streamwise location, were used to generate the interacting vortices. The wings were mounted in disks, which, in turn, were mounted in circular holes in the side of the test section, permitting changes in the wing angle of attack.

In all, four different types of models were used. The primary type used for the merging distance measurements, and the only type used as generators for rolling moment and hot-wire anemometer velocity measurements were NACA 0012 6-in.-chord rectangular wings with 4-in.-span elliptical tips. To determine the best nondimensional parameters to be used in the functional relationship between merging distance and vortex spacing, two other model types with smaller chords were used. The first type had a 0012 airfoil, but a simple rectangular planform and a 5-in. chord. The second type was also rectangular, but with a 0015 airfoil and a 4-in. chord. To obtain merging data at relatively high values of centerline circulation Γ_0, 1.5-in.-chord full-span rectangular external airfoil flaps, set at 20-deg deflection, were attached to the trailing edge of the 5-in.-chord models. As a further test of the nondimensional parameters, merging distance data were taken with the wings inserted through opposite walls as

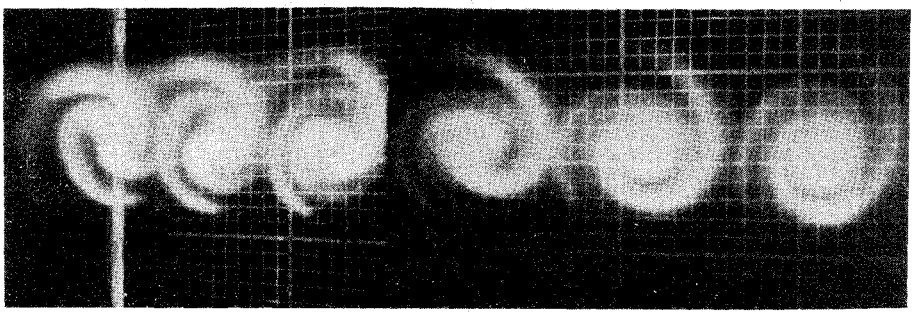

Fig. 2 Merging sequence illuminated by light slits.

well as through adjacent walls, thus permitting a comparison between two cases with identical vortex spacing, chord, and angle of attack, but differing values of span, d_c, and Γ_0. In addition to the four models used as vortex generators, a 10-in.-span, 2.5-in.-chord, 0015 rectangular wing model was used as a follower model, to measure rolling moments induced by the trailing vortices. Additional information on model and wind tunnel characteristics, as well as error limits on data obtained, can be found in Ref. 17.

Merging Distance Measurements

Measurement of merging distances, obtained at maximum tunnel speed, consisted of setting the pair of wing models in use at the time to a given value of span and angle of attack, then recording the distance downstream of the wings where the vortices merged. A given angle of attack would be selected and maintained throughout a series, then the semispans varied to achieve different initial vortex spacings. Since varying the models' spans and the secondary effect of changing both Γ_0 and d_c, the spans were always kept equal to ensure identical vortices.

The identification of the point of merger is somewhat arbitrary. With the type of flow visualization used, the cores of the vortices show up in the light slits as holes, where no steam is present, surrounded by areas of fairly dense steam. As the light slit is moved downstream, these clear centers can be seen to rotate about each other and move closer together. At some streamwise point, which was chosen as the merger point, two separate clear centers cease to exist, leaving either a single clear area or no clear space at all. The best means of accurately locating this point is to sweep a single light slit rapidly downstream. The rotation of the two cores about each other is always easy to see with this method, and the point where this motion ceases because the cores have merged can be picked up immediately. Two or three sweeps are usually sufficient to pinpoint the merger point to within an inch.

Velocity and Rolling Moment Measurements

The twin hot-wire anemometers connected to a two-wire probe were used to measure vortex tangential and axial flow velocity components at various points in the merging process. Traverses of the flow were made for several vortex configurations in such a manner that the hot-wire probe passed horizontally through the center of the vortex.

The follower model and sting balance were used to measure the rolling moment hazard of various vortex configurations. Steam and liquid nitrogen flow visualization was used to help center the model on the vortex. Fine position adjustments were made by moving the model small increments in lateral position until the maximum rolling moment was measured. Both single and merged twin-vortex systems generated by the elliptically-tipped models were studied to obtain a measure of the hazard attenuation associated with the merging process.

Qualitative Characteristics of Vortex Interaction

The first phase is initial roll up, the period from the time the flow passes the wing until the vortex is completely formed. The clear center in this phase first appears in each vortex about a half-chord-length downstream of the wingtip and rapidly grows in one or two semispans to the size it maintains throughout the rest of the process until the merger point is reached. The end of this phase is taken to be the point where the diameter of the clear hole has reached its limiting value. When two models placed in opposite or adjacent walls had their tips close enough together, merger would occur in approximately the same distance as rollup, so that although two separate vortices began to roll up independently, only a single vortex remained when rollup was complete.

The second phase of the merging process has the vortices separated by a distance at least twice as great as the peak velocity core diameters, which in this study means center-to-center distances greater than 2 in. During this phase the clear centers remain nearly circular, suggesting that little distortion of the vortex cores is occurring. The vortices spiral around each other as they move downstream and their separation distance gradually decreases. This phase ends when separation distance decreases to the previously described lower limit and significant distortions of the vortex cores begin to show.

The third phase covers the period from the point where the vortex cores begin to show distortions in shape until the merger point is reached. This region is seldom longer than twice the length of the rollup region, although length depends on the observer's judgment of when "significant" core distortion has occurred. Whereas the first two phases have quite steady flow characteristics, this third phase is much more unsteady. The merger point location is relatively steady, but the angular orientation of the two vortices at fixed, small distances upstream of the merger point may change rapidly with time, as much as 180 deg, indicating small but rapid changes in vortex spacing. Clear centers immediately upstream of the merger point have markedly quasielliptical shapes with major to minor axis ratios of nearly two just before merger. The major axes of these distorted cores are oriented approximately perpendicular to the line connecting the vortex centers.

The final phase encompasses the region downstream from the merger point. At the merger point, the two separate, clear centers distinguishable up to this point disappear. There may be no similar clear area in the merged vortex for a short space, then a single, smaller space reforms. Once the single merged vortex begins forming, the flow becomes quite steady once more, and a layering of the water droplets outside the clear center is visible, indicating a single structured vortex has reformed. At lower Reynolds number, as well as in the current tests, flow visualization has shown that the merged vortex initially consists of a nested pair of spiral sheets, with each of the pair of sheets retaining separate identity very close to the center.[9]

Figures 3a and b, with flow from left to right, illustrate the four phases of the merging process. Steam has been inserted through the tunnel inlet, and in Fig. 3a cross sections of the merging vortices are shown by means of a series of ten light slits. In Fig. 3b, another view of merging with five light slits is shown in which the formation of the clear center downstream of the merging point is visible. The nesting of the pair of

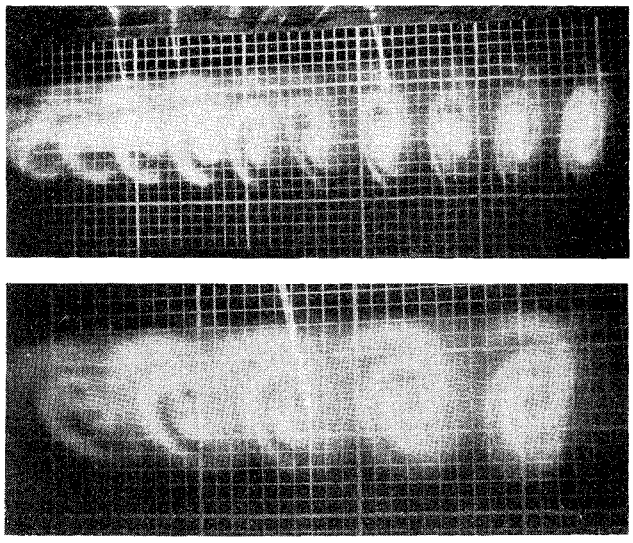

Fig. 3 Two views of merging.

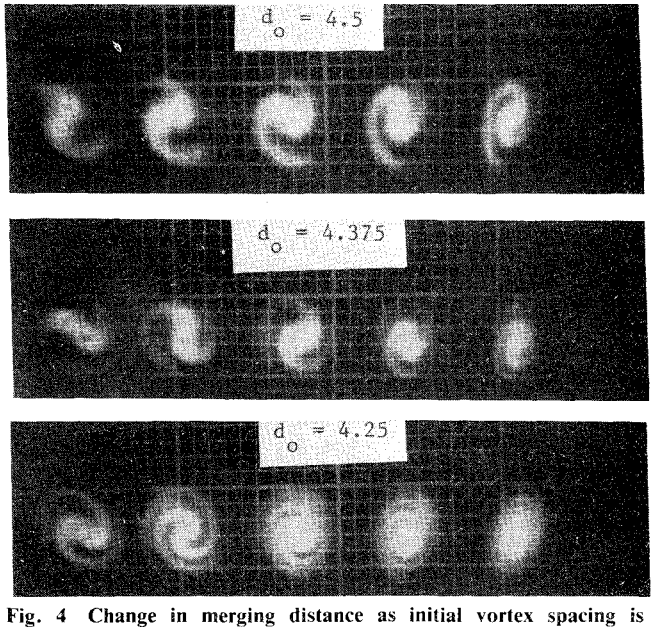

Fig. 4 Change in merging distance as initial vortex spacing is reduced.

sheets is also visible in the downstream cross sections. Farther downstream the steam diffuses to appear more like the usual single vortex.

The previous discussion of the four phases of the merging process presupposes two equal-strength like-sense vortices rolling up at a moderate initial separation distance from wing models at the same streamwise location. The apparent effect of reducing initial vortex separation is to shorten phase two only until critically small initial spacings are reached, where phases one, two, and three are combined as previously described in a merging rollup phase. Using light-slit illumination. Fig. 4 illustrates the effect of reducing initial vortex spacing in 1/8-in. increments for the 6-in.-chord elliptically-tipped models. The forward movement of the merger point is obvious. With the entire test section lighted, Fig. 5 illustrates the increase in rotation rate as separation distance is reduced. Merger has taken place in the bottom photograph. The two original vortices can be seen at the left just prior to merger.

A second modification of the merging process occurs when the vortices are not of equal circulation strength. The effect of leaving the angle of attack of one wing constant at 15 deg,

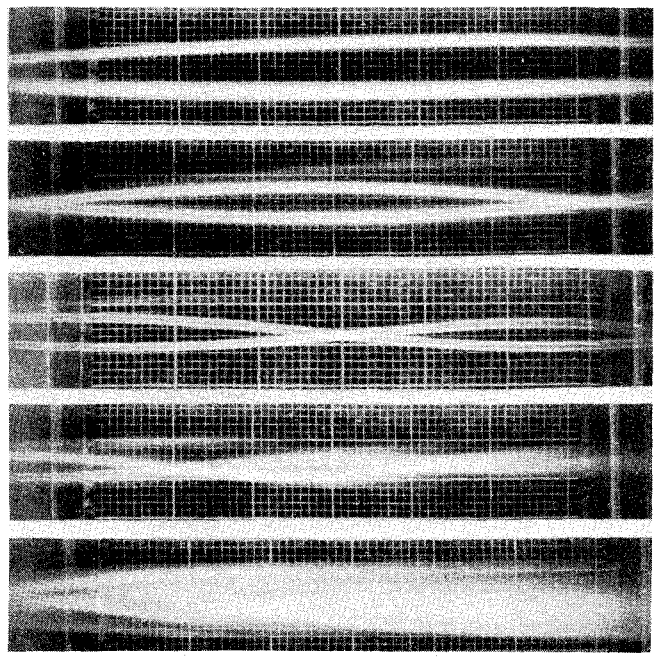

Fig. 5 Vortex behavior as initial vortex spacing is decreased until merging occurs.

while reducing the other to 13, then 11, and finally 9 deg without changing vortex spacing, is illustrated in Fig. 6. As can be seen, the merger point moves forward and the weaker vortex is quickly dominated by the stronger one. It also becomes apparent that the merger point is much more difficult to determine for unequal vortex strength, because the stronger vortex never really disappears. It is for this reason that merging distances were only measured for equal-strength vortices. When the angle of attack of one model was reduced further to -15 deg, two equal-strength opposite-signed vortices were produced similar to the vortex pair created by a simple finite wing. Similar flow visualization photographs of unequal-strength vortices are shown in Ref. 9, with qualitatively similar results, except for small differences with the current results since the vortices shown in Fig. 5 are an order of magnitude stronger in circulation than those of Ref. 9.

All measurements and observations in this study were made over a relatively limited range of Reynolds numbers ($1.2\times10^5<\Gamma_0/\nu<4.6\times10^5$ and $3.9\times10^5<Uc/\nu<6.3\times10^5$). As a result, it would not be totally unexpected if some details of the merging process change at much higher Reynolds numbers. It was observed, however, that lowering wind tunnel velocity did not appreciably change the merging point, so that the effect of Reynolds number on merging distance is small in the range of Reynolds number quoted above and those somewhat lower. There could be large effects due to changes in Reynolds number, of course, from those of the current tests to flight Reynolds numbers that are an order of magnitude to two larger.

Merging Distance Criteria

If the time (or streamwise distance) measured from formation of two equal-strength, corotating vortices to the point of merging into a single vortex is assumed to be only a function of vortex strength Γ_0, initial separation distance d_0, and core diameter d_c, then

$$t\Gamma_0/d_c^2=f(d_0/d_c) \tag{2a}$$

or

$$x_m\Gamma_0/U_\infty d_c^2=f(d_0/d_c) \tag{2b}$$

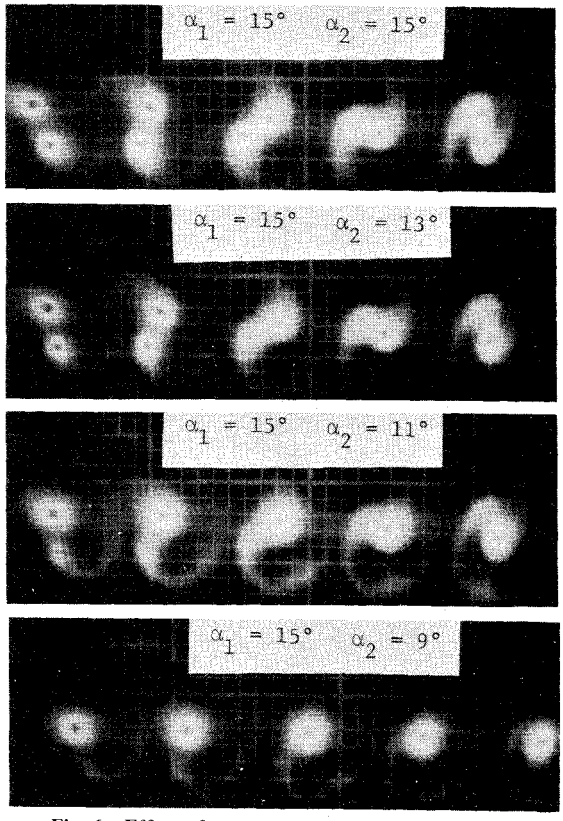

Fig. 6 Effect of reducing Γ_2 with Γ_1 and d_0 fixed.

Unless the core diameter d_c is in some way related to the circulation profile, the use of Eq. (2) presupposes no relationship between merging distance x and the specific circulation profile in the vortex core. The success of the equivalent Rankine circulation defect diameter d_Γ, or angular momentum-defect d_M, which are functions of the specific profile, in coalescing Rossow's merging boundaries and in reconciling his result with Christiansen's makes d_Γ and d_M attractive normalizing diameters. The defect diameters were calculated from the inviscid Betz vortex circulation profile[18] for the given wing geometry. Therefore, functional relationships that account for the effect of wing geometry on vortex circulation profile are

$$x_m\Gamma_0/U_\infty d_\Gamma^2 = f(d_0/d_\Gamma) \tag{3a}$$

or

$$x_m\Gamma_0/U_\infty d_m^2 = f(d_0/d_m) \tag{3b}$$

The initial vortex spacing d_0 was predicted from wing geometry and relative position of the two wings, using the spanwise locations of the vortices predicted by the Betz method. The results of the experiments plotted in terms of Eqs. (3a) and (3b) are shown in Ref. 19. Although the data correlate fairly well using Eqs. (3a) or (3b), it was found that, of all the numerous combinations of normalizing distances attempted, the best are

$$x_m\Gamma_0/U_\infty bc = f(d_0/d_\Gamma) \tag{4a}$$

and

$$x_m\Gamma_0/U_\infty S = f(d_0/d_m) \tag{4b}$$

The experimental values of merging distance plotted using Eq. (4a) are illustrated in Fig. 7. The equivalent core diameters d_Γ and d_M, calculated on the basis of an inviscid profile, do not account for the effect of the viscous inner core. Equation (4) is an improvement over Eq. (3), probably because the size of the inner core depends partially on momentum loss within the wing boundary layer,[20] which is a function of the chord length c. The inviscid circulation profile was used to calculate d_Γ and d_M, rather than the actual profile, since experiments showed that the profile close to the wing is close to the Betz profile, except for the viscous core, where there is as yet insufficient information available.

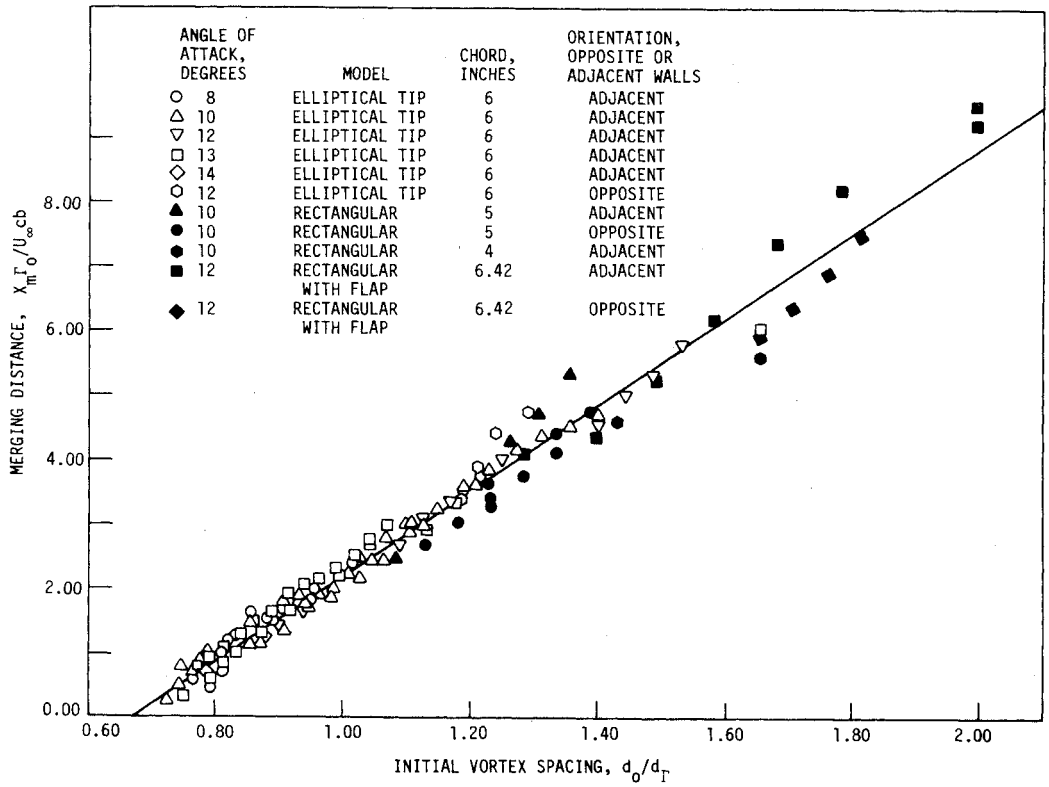

Fig. 7 Variation of merging distance with initial vortex spacing for various model configurations (Eq. 4a).

The linear nature of the curve in Fig. 7 is interesting, since an infinite merging distance is predicted by the two-dimensional inviscid calculation for $d_0/d_\Gamma = 1.7$. Once this linear trend was perceived, an effort was made to approach this merging boundary. Since test section length was limited, higher values of Γ_0, through the use of flaps and smaller values of c, b, and d_Γ through the use of smaller generating models, offered the only means of operating in this region of the curve. As can be seen from Fig. 7, merging was achieved for values of d_0/d_Γ of 1.99, outside Rossow's and Christiansen's merging boundary. Also, the data do not appear to depart significantly from the linear curve, although the scatter and sparsity of data in this region could mask the beginning of a nonlinear trend. The attainment of merging a small amount outside the merging boundaries would not in itself be proof that merging can be achieved well outside the boundaries. The data plotted in terms of the momentum defect diameter d_M do not reach the inviscid merging boundary as predicted by that normalization, so whether an inviscid merging boundary for a Betz-type vortex was exceeded or not remains to be seen. More inviscid calculations for a wider variety of vortex types or experiments in longer wind tunnel test sections are needed before this can be determined. (Not only are the experimental circulation profiles quite different from those used in Rossow's calculations, but the vorticity fields of the two experimental vortices usually overlapped, although in regions of very low vorticity; in the inviscid calculations, the initial vorticity fields were not allowed to overlap.)

The linearity of the curve and the fact that it shows little sign of changing this trend are evidence that merging of real vortices can possibly be expected outside the inviscid two-dimensional merging boundaries. This result would not negate the importance of inviscid two-dimensional calculations but would rather illustrate the action of viscosity and turbulence and possibly three-dimensional effects. Also, merging distance goes to zero for $d_0/d_\Gamma = 0.668$ rather than zero. For initial spacings less than 0.668, the vortices do not roll up independently, but rather roll up already merged. The straight line drawn through the data is the linear least-squares fit of all the data points weighted equally:

$$(x_m\Gamma_0/U_\infty cb) = (6.69d_0/d_\Gamma) - 4.47 \qquad (5)$$

It should be noted that, in extending the wind tunnel test section length from 6 to 28 ft, it was necessary to construct the extension as a constant area section. As a result, because of the boundary-layer growth on the test section walls, the effective tunnel area decreases with downstream distance, and freestream tunnel speed increases about 5% in the first 22 ft of test section. Thus, the time from vortex formation is not quite x_m/U_∞ but $\int dx/U_\infty(x)$. The values of x_m/U_∞ used in reducing the data presented are thus actual values of time, calculated using the integral. It is not known what effect the flow acceleration has on vortex interaction, but it is suspected to be small, since flow pattern did not appreciably change as the tunnel speed control was changed.

Three-dimensional effects, mentioned above and neglected in Christiansen's and Rossow's work, have been discussed by Hackett and Evans.[21] They stated that for two corotating vortices, one effect of self-induced velocity due to vortex curvature is to retard the rate of rotation of the line connecting the vortex centers. Also, the tipping of the vortex axes relative to the streamwise axis produces velocity components in the downstream direction in the region between the vortices. This effect, which they call axial pumping, is also felt on the vortices themselves, thus stretching the vortices and further reducing the apparent rate of their relative rotation. As the result of these two effects, a purely two-dimensional calculation of the period of rotation results in a shorter wavelength of the spiral motion than that obtained by three-dimensional calculation. Since they found time-to-converge to be highly dependent on wavelength, two-dimensionally derived wavelengths produced erroneous predictions of time-to-converge, even though the balance of their computation was three-dimensional.

The current results for a merging distance criterion are for identical vortices of equal strength. For the more practical situation where multiple vortices are shed from each semispan of a flapped wing, the situation is more complicated. Even for just two vortices of differing strengths Γ_1 and Γ_2, a merging distance equation would have to be of the form

$$\frac{x_m\Gamma_1}{U_\infty d_{\Gamma_1}^2} = f\left(\frac{d}{d_{\Gamma_1}}, \frac{d_{\Gamma_1}}{d_{\Gamma_2}}, \frac{\Gamma_1}{\Gamma_2}\right) \qquad (6)$$

Since it is difficult to define a merging distance experimentally with the visual technique described earlier for vortices of much differing strengths, it is hoped that merging distance criteria such as Eq. (6) can eventually be determined at least partially with the aid of finite-difference calculations.

Corsiglia and Orloff[22] have made estimates of multiple-vortex circulation strengths and circulation profiles from wind tunnel experiments on a flapped jet-transport model. Ciffone and Lonzo[23] presented flow visualization data for a similar model in a tow tank from which estimates of merging distance were made for those cases in which wingtip and flap vortices appeared to merge. Two configurations are of interest. In the first, both inboard and outboard flaps are deployed. The two vortices, shed on each semispan from the wingtip and from the outboard edge of the outboard flap, merge fairly quickly within 1-4 spanlengths downstream,[22,23] since their separation distance is small. In the second configuration, only the inboard flap is deployed. The tip vortex and that shed from the outboard edge of the inboard flap merge considerably farther downstream (13 spanlengths or greater), since their initial separation distance is 2.4 times larger.[22] Values of circulation defect diameter for each vortex were calculated from Corsiglia and Orloff's data. For each configuration, the values of diameter d_Γ and circulation Γ for the two vortices were averaged and merging distance calculated from Eq. (5). The calculated values of merging distance of 1.2 spans for the first configuration and 25 spans for the second agree qualitatively with the observed values. The calculated values could not be expected to be very accurate, however, since the tip and flap vortex strengths differ considerably for both cases.

Premerger Vortex Interaction

The relative separation distances and angular positions of two interacting vortices were measured by visual observation prior to merger. The values of θ, the absolute angle of the line connecting the vortex centers relative to the first horizontal orientation of this line, versus time from generation are plotted for the five cases studied in Fig. 8a. The smooth curves drawn on the figure are least-squares fits of the data subsequently used to obtain $d\theta/dt$ for circulation predictions. Figure 8b shows the vortex separation distance data, together with polynomial curves through the points used for the circulation predictions. Figure 8 also includes scaled results taken from Rossow's two-dimensional inviscid calculations.[14]

Table 1 contains the maximum circulation values predicted for the vortices from the $d\theta/dt$ and d data using the formula $d\theta/dt = \Gamma/\pi d^2$. Also listed for each case is the value of Γ for that radial distance predicted from wing geometry and theory. In most cases, the rotation rate circulation predictions are less than the Betz values. This is to be expected for reasons set forth by Evans and Hackett.[24] From their data, using the spiral angle measured on Fig. 4, a 3% reduction in predicted circulation could be expected from the vortex stretching due to axial pumping. A further reduction could be expected from the self-induced velocity due to vortex curvature, although this was not quantified in their report. By predicting Γ from vortex motions at various values of d, a circulation profile for

Table 1 Circulation predictions from vortex motions

Model	Half-span, in.	Angle of attack, deg	Total circulation, ft^2/sec	Maximum predicted circulation Γ/Γ_0	Betz circulation, Γ/Γ_0
Flapped rectangular	11.0	12	150.121	0.91	0.93
Elliptical tip	14.0	10	85.3	0.815	0.87
Elliptical tip	13.75	10	84.9	0.86	0.85
Elliptical tip	14.0	10	85.3	0.816	0.84
Elliptical tip	13.0	10	80.6	0.76	0.87

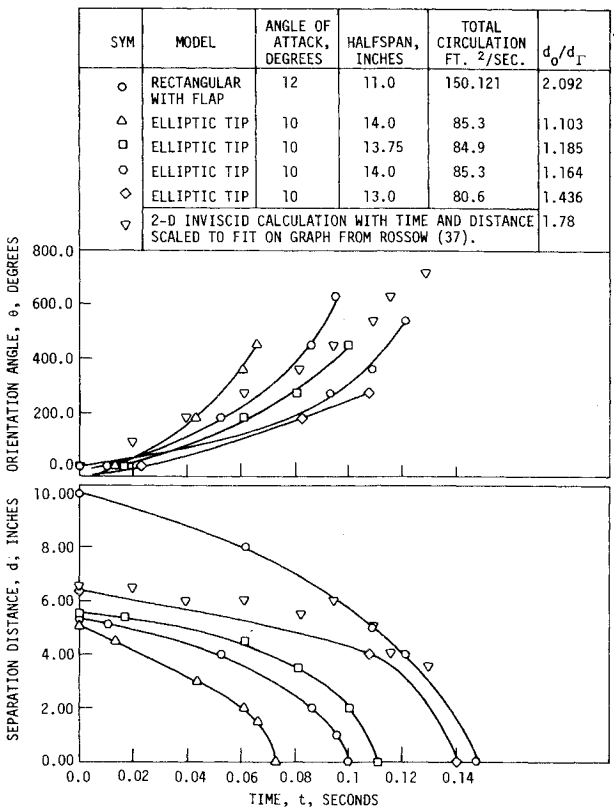

Fig. 8 Vortex motions prior to merging.

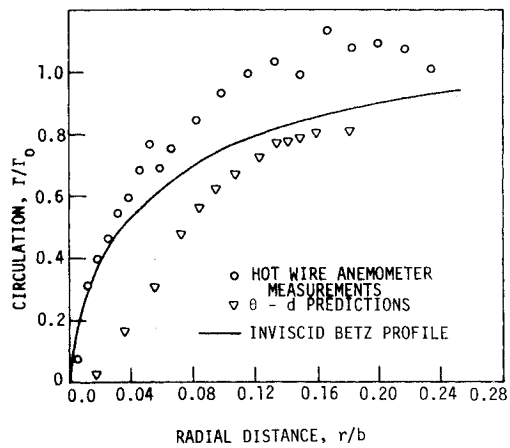

Fig. 9 Comparison of measured, predicted, and ideal vortex-circulation profiles.

the vortex can be predicted. Since the motion of each vortex center is caused by the circulation at that distance from the companion vortex, at least in a two-dimensional approximation, the separation distance is equal to the radial distance r, for which the particular Γ is predicted. Thus, the Γ vs d profile is also a Γ vs r profile and can be compared with the ideal Betz profile and the Γ profile measured with the hot-wire anemometer. This is done in Fig. 9. As can be seen, the ratio of predicted to measured circulation decreases with separation distance. This is to be expected, since decreasing d increases both vortex curvature and spiral angle, resulting in greater three-dimensional effects. The error due to ignoring the entire vorticity field in calculating the motion of each vortex center becomes more pronounced as the separation distance d decreases.

Hot-Wire Anemometer Velocity Measurements

Figure 9 also shows a circulation profile measured with the hot-wire anemometer probe for a trailing-vortex shed from one of the elliptically tipped models at a 10-deg angle of attack and with a 15-in. span. Included for comparison are the profile predicted from wing geometry using the Betz method and the profile predicted from vortex motions. The measured circulation values differ in two ways from the Betz profile. First, maximum circulation is achieved for a smaller radial distance than for the Betz profile. Second, this maximum value is slightly greater than the predicted value of Γ_0. This circulation overshoot is only about 10% and could be the result of experimental error. Since the overshoot occurs at fairly large radial distances, quite small errors in measuring tangential velocity would produce large errors in circulation values. Since tangential velocities are determined by taking the difference of the two anemometer voltages, and these voltages are very nearly equal at these large radial distances, the chance for error in these values is further increased. Errors arise not only from probe interference, but also because the hot-wire profiles represent only one traverse through the vortex to its center. Eventually, more complete flowfield surveys will be made that will show the deviation from axisymmetry. Nonetheless, circulation overshoot is predicted by Saffman and Govindaraju[25] at certain stages in turbulent vortex decay, so the measured overshoot may be real. The peaking and leveling off of the circulation values at a smaller radial distance than predicted by the Betz method could indicate that the vortex is beginning to transform from a primarily inviscid profile to a self-similar profile as predicted by Iversen.[26] At downstream distance of 252 in., the single vortex is about at the downstream end of the plateau region, as defined by Ciffone and Orloff[27] and Iversen.[28]

Figure 10 shows the tangential velocity and circulation profiles for three vortex configurations, superimposed for comparison. The first profile is for a single vortex generated by a single wing at a 10-deg angle of attack; the second profile is for two merging vortices from wings at a 10-deg angle of attack measured at the merging point; and the third is for the same vortices well downstream of merger. As can be seen, at large radius the merged vortices contain twice the circulation of the single vortex but never exhibit higher tangential velocities. These results, plus the fact that turbulence in the merged vortex is higher than in the unmerged vortices,[10,29] leading to more rapid decay, demonstrate the hazard-attenuating capabilities of the merging process.

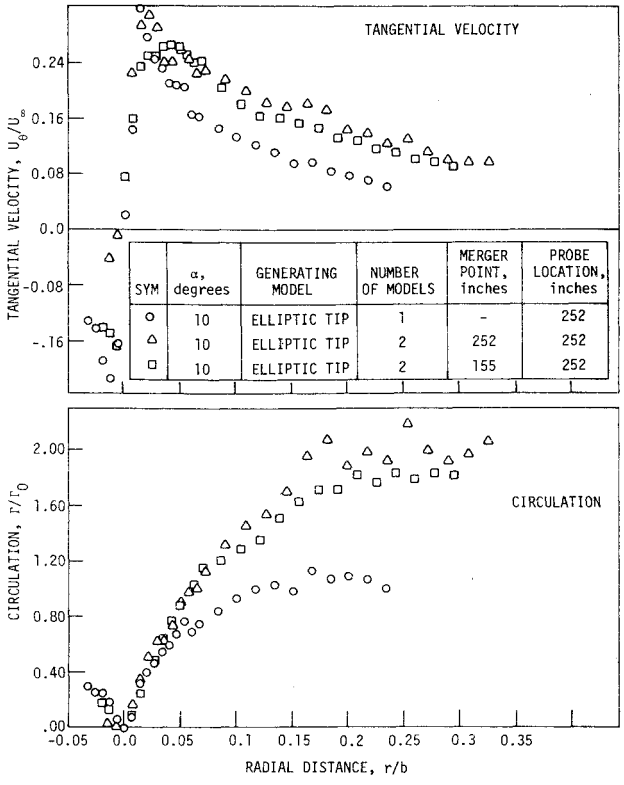

Fig. 10 Comparison of velocity and circulation profiles for single and merged vortices.

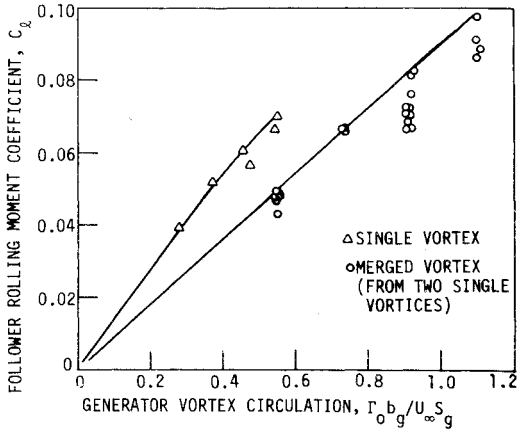

Fig. 11 Variation of follower rolling moment with vortex circulation.

Rolling-Moment Measurements

The data obtained from the rolling-moment model are shown in Fig. 11, which is a plot of the follower rolling moment coefficient c_l against the nondimensional parameter $\Gamma_0 b_g/U_\infty S_g$, which is proportional to the generator lift coefficient C_L. As can be seen, the curves are essentially linear, although some scatter is present, and the curve for single vortices is considerably higher than that for merged vortices, indicating the relative reduction in hazard.

The scatter observed in the data can be attributed to failure to position the follower in the exact center of the vortex. Most of the lower points should not be considered, since they do not represent the maximum hazard measured. Therefore, the straight lines are drawn on the graph nearer the maximum values at each point.

Conclusions

The merging distance curve shown in Fig. 7 represents remarkable correlation of data considering that the data were obtained entirely by flow visualization. The coalescence of data in the correlation curve illustrates the utility of the circulation defect diameter or angular momentum defect diameter in accounting for variations in vortex circulation profile shape. The circulation defect diameter and angular momentum defect diameter are also shown to be effective in correlating the inviscid merging boundaries calculated by Rossow.[14] The diameter d_Γ seems to work slightly better in the correlation of merging distance, whereas the core diameter d_M is slightly superior for the coalescence of inviscid merging boundary calculations.

If the two-dimensional inviscid merging boundary were strictly applicable to real flows, the merging distance curve should approach a vertical asymptote at a separation distance d/d_Γ or d/d_M of approximately 1.7. Instead, the experimental curve remains linear through to the largest value of d/d_Γ obtained experimentally—(1.99). Thus, viscosity effects and possible three-dimensional effects cause merging outside of the separation distance range predicted by the use of d_Γ in correlating the aforementioned inviscid calculation. Knowledge of whether the inviscid merging bounda y for Betz-type vortices has indeed been exceeded experimentally will exist only after further experiments and/or inviscid calculations have been performed.

Comparison of tangential velocity profiles for single and merged vortices shows that, although the merged vortex formed from two equal-strength vortices, each of strength Γ_0, contains twice the large radius circulation as a single vortex of strength Γ_0, the peak tangential velocity of the merged vortex is no greater than the peak velocity of the single vortex. Due to a merged vortex, rolling moment measurements on a following model show a sizable hazard attenuation associated with the merging process. The rolling moment due to the merged vortex on a follower model was independent of merging distance over the range of values studied.

Acknowledgment

This research is supported by the NASA Ames Research Center, and the Iowa State University Engineering Research Institute. The assistance of R. Brickman and D. Backhus in a portion of the experimental work is gratefully acknowledged.

References

[1] Dunham, R.E. Jr., "Exploratory Concepts Found to be Unsuccessful for Aircraft Wake Vortex Minimization," *NASA Symposium on Wake Vortex Minimization*, Washington, D.C., 1976, pp. 218-257.

[2] Corsiglia, V.R. and Dunham, R.E. Jr., "Aircraft Wake-Vortex Minimization by Use of Flaps," *NASA Symposium on Wake Vortex Minimization*, Washington, D.C., 1976, pp. 303-336.

[3] Jacobson, R.A. and Barber, M.R., "Flight Test Technique for Wake Vortex Minimization Studies," *NASA Symposium on Wake Vortex Minimization*, Washington, D.C., 1976, pp. 191-217.

[4] Winant, C.D. and Browand, F.K., "Vortex Pairing: The Mechanism of Turbulent Mixing-Layer Growth at Moderate Reynolds Number," *Journal of Fluid Mechanics*, Vol. 63, April 1974, pp. 237-255.

[5] Browand, F.K. and Weidman, P.O., "Large Scales in the Developing Mixing Layer," *Journal of Fluid Mechanics*, Vol. 76, July 1976, pp. 127-144.

[6] Moore, D.W. and Saffman, P.G., "Structure of a Line Vortex in an Imposed Strain," *Aircraft Wake Turbulence and its Detection*, Plenum Press, New York, 1971, pp. 339-354.

[7] Moore, D.W. and Saffman, P.G., "The Density of Organized Vortices in a Turbulent Mixing Layer," *Journal of Fluid Mechanics*, Vol. 69, June 1975, pp. 465-473.

[8] Bilanin, A.J., Snedeker, R.S., and Teske, M.E., "Interaction and Merging of Line Vortices," unpublished manuscript, Aeronautical Research Associates of Princeton, Princeton, N.J., 1976.

[9] Bilanin, A.J., Snedeker, R.S., and Teske, M.E., "Interactions and Merging of Line Vortices," U.S. Air Force Office of Scientific Research, AFOSR-TR-76-0873, 1976.

[10] Bilanin, A.J., Teske, M.E., Donaldson, C. duP., and Snedeker, R.S., "Viscous Effects in Aircraft Trailing Vortices," *NASA Sym-*

posium on Wake Vortex Minimization, Washington, D.C., 1976, pp. 55-122.

[11] Roberts, K.V. and Christiansen, J.P., "Topics in Computational Fluid Mechanics," *Computer Physics Communications, Supplement*, Vol. 3, Sept. 1972, pp. 14-32.

[12] Christiansen, J.P., "Numerical Simulation of Hydrodynamics by the Method of Point Vortices," *Journal of Computational Physics*, Vol. 13, Nov. 1973, pp. 363-379.

[13] Christiansen, J.P. and Zabuski, N.J., "Instability, Coalescence and Fission of Finite-Area Vortex Structures," *Journal of Fluid Mechanics*, Vol. 61, Nov. 1973, pp. 219-243.

[14] Rossow, V.J., "Convective Merging of Vortex Cores in Lift-Generated Wakes," *Journal of Aircraft*, Vol. 14, March 1977, pp. 283-290.

[15] Rossow, V.J., "Inviscid Modeling of Aircraft Trailing Vortices," *NASA Symposium on Wake Vortex Minimization*, Washington, D.C., 1976, pp. 4-54.

[16] Steger, J.L. and Kutler, P., "Implicit Finite-Difference Procedure for the Computation of Vortex Wakes, *AIAA Journal*, Vol. 15, April 1977, pp. 581-590.

[17] Brandt, S.A., "Interaction and Merging of Aircraft Trailing Vortices," Master of Science Thesis, Iowa State University, Ames, Iowa, 1976.

[18] Rossow, V.J., "On the Inviscid Rolled-Up Structure of Lift Generated Vortices," *Journal of Aircraft*, Vol. 10, Nov. 1973, pp. 647-650.

[19] Iversen, J.D., Brandt, S.A., and Raj, P., "Merging Distance Criteria for Co-rotating Trailing Vortices," Proceedings, Conference on Aircraft Wake Vortices, U.S. Dept. of Transportation, Transportation Systems Center, Cambridge, Mass., 1977.

[20] Bilanin, A.J. and Donaldson, C. duP., "Estimation of Velocities and Roll-Up In Aircraft Vortex Wakes," *Journal of Aircraft*, Vol. 12, July 1975, pp. 578-585.

[21] Hackett, J.E. and Evans, P.F., "Numerical Studies of Three-Dimensional Breakdown in Trailing Vortex Wakes," AIAA Paper 76-416, San Diego, Calif., 1976.

[22] Corsiglia, V.R. and Orloff, K., "Scanning Laser-Velocimeter Surveys and Analysis of Multiple Vortex Wakes of an Aircraft," NASA TM-X-73, 169, 1976.

[23] Ciffone, D.L. and Lonzo, C. Jr., "Flow Visualization of Vortex Interactions in Multiple Vortex Wakes Behind Aircraft," NASA TM X-62, 459, 1975.

[24] Evans, P.F. and Hackett, J.E., "Numerical Studies of Three Dimensional Breakdown in Trailing Vortex Wakes," NASA CR-137888, 1976.

[25] Saffman, P.G. and Govindaraju, S.P. "Flow in a Turbulent Trailing Vortex," *Physics of Fluids*, Vol. 14, Oct. 1971, pp. 2074-2080.

[26] Iversen, J.D., "Inviscid to Turbulent Transition of Trailing Vortices," AIAA Paper 75-883, Hartford, Conn., 1975.

[27] Ciffone, D.L. and Orloff, K.L., "Far Field Wake Vortex Characteristics of Wings," *Journal of Aircraft*, Vol. 12, May 1975, pp. 464-470.

[28] Iversen, J.D., "Correlation of Turbulent Trailing Vortex Decay Data," *Journal of Aircraft*, Vol. 13, June 1976, pp. 338-342.

[29] Bilanin, A.J., Teske, M.E., and Williamson, G.G., "Vortex Interactions and Decay in Aircraft Wakes," *AIAA Journal*, Vol. 15, Feb. 1977, pp. 250-260.